Water and Wastewater, Vol. 37, No. 6, pp:

Probabilistic Seismic Loss Estimation for Vulnerable Water System Components in Kashan, Iran through Fragility Functions

Hossein Tahghighi[1*], Issa Ilyati[2]

1. Assoc. Prof., Dept. of Civil Engineering, Faculty of Engineering, University of Kashan, Kashan, Iran
(Corresponding Author) tahghighi@kashanu.ac.ir
2. PhD. Student, Dept. of Earth Sciences, Faculty of Science, Shiraz University, Shiraz, Iran

https://doi.org/10.22093/wwj.2026.578675.3544 **Original Paper**

Abstract

Water systems are indispensable for effective crisis management; however, they are highly vulnerable to the devastating impacts of earthquakes. This study assesses the seismic vulnerability of critical water system components in Kashan, Iran, including wells, storage tanks (ground supported and elevated), and pump stations, and provides quantitative loss estimates for two earthquake scenarios: Design Basis Earthquake and Maximum Considered Earthquake. Field surveys characterized the spatial distribution, capacity, classification, and operational status of all components. Direct physical damages were quantified using empirical HAZUS fragility functions for most components and analytical functions for elevated tanks. The risk analysis incorporates crucial modification factors accounting for seismic design levels and observed asset degradation, integrating probabilistic ground motion fields to generate loss maps. Key findings reveal that elevated tanks are the most vulnerable, with their Compounded Damage Ratio rising from 0.421 under DBE to 0.680 under MCE, and complete damage probability reaching 32.1%. MCE events mainly cause severe structural damage, while DBE events typically result in slight to moderate damage. On ground tanks, pump stations, and wells have DRc values of 53.3%, 50.2%, and 29.2% under MCE, respectively. The significant vulnerability of unanchored components and aging infrastructure underscores the urgent need for targeted mitigation measures, including seismic anchorage, retrofitting, or complete reconstruction where necessary. These recommendations offer actionable and practical guidance for enhancing the safety, reliability, and overall resilience of water systems in earthquake prone regions, contributing to improved disaster preparedness and response capabilities.

Keywords:
Seismic Vulnerability,
Water System,
Earthquake Hazard,
Fragility Analysis,
Risk Assessment,
Kashan.

Received. Mar. 25, 2026
Revised: May 23, 2026
Accepted: July 28, 2026

To cite this article:
Tahghighi, H., Ilyati, I., 2027. Probabilistic seismic loss estimation for vulnerable water system components in Kashan, Iran through fragility functions. *Water and Wastewater*, 37(6), https://doi.org/10.22093/wwj.2026.578675.3544.

1. Introduction

Disruption of lifelines, such as utility networks, caused by external hazards has profound consequences for both immediate public safety and long-term socioeconomic stability (Pitilakis et al., 2008). Among utility networks, water systems are especially critical because they support fire-fighting, sanitation, and basic household needs; any interruption can therefore amplify the impacts of a disaster. A large body of post-event investigations has shown that water system components are among the most vulnerable elements during strong ground shaking. The 1906 and 1989 California earthquakes, for instance, exposed severe weaknesses in water supply infrastructure, leading to widespread fires and prolonged service outages (Eidinger et al., 2006).

In Iran, the 2003 Bam earthquake devastated wells, storage tanks, and transmission pipelines (Eshghi et al., 2004). Similar patterns of persistent damage were observed after the 2004 Niigata (Japan) and 2009 L'Aquila (Italy) earthquakes (Scawthorn et al., 2006; Esposito et al., 2013). Most recently, the 2023 Türkiye-Syria earthquakes inflicted catastrophic damage on water supply facilities, leaving more than 14 million people without reliable water access and triggering massive recovery operations (Toprak et al., 2025). These events collectively underscore that the seismic resilience of water system lifelines remains insufficient, and their interdependencies with other critical infrastructures exacerbate overall disaster impacts.

Early attempts to quantify seismic performance of utility networks were pioneered by the National Institute of Building Sciences (FEMA, 1997). Building on this foundation, the Mid-America Earthquake Center proposed a probabilistic approach that explicitly accounted for component interdependencies within lifeline networks (Kim et al., 2007). In the Middle East, the Japan International Cooperation Agency[1] carried out a three-phase vulnerability study of Tehran's water supply system, producing an earthquake-resistant design plan that addressed both pipe networks and point facilities (JICA, 2006). Pitilakis et al., (2006) later refined these concepts through the RISK-UE methodology, integrating seismic hazard assessment with component-level fragility modeling to generate system-wide risk estimates.

Subsequent research has focused on improving the spatial representation of ground motion fields; Abbasnejadfard et al., (2020) and Wen and Bi, (2025) developed correlation functions for Peak Ground Acceleration[2] and Spectral Acceleration[3], thereby enhancing the fidelity of risk analyses for distributed infrastructure. Beyond shaking, proximity to active faults introduces additional failure mechanisms due to surface rupture and ground deformation (Tahghighi, 2011; Melissianos et al., 2024). Several studies have documented severe damage to underground tunnels, pipelines, and other lifeline systems when fault rupture intersected the infrastructure (Ghadimi Chermahini and Tahghighi, 2019; Li and Ni, 2025; Toprak et al., 2026).

In a recent study, Ilyati and Akbari, (2024) assessed flood risk zoning for vulnerable components of the water supply system in Kashan, identifying 22 wells and 7 storage tanks at risk, which underscores the importance of multi-hazard risk assessment for the city's water infrastructure. Seismic risk assessments for utility systems depend on the probabilistic combination of vulnerability models for the various components and subcomponents (Pitilakis and Argyroudis, 2014). A substantial portion of the existing literature concentrates on pipe network fragilities (e.g., Fragiadakis et al., 2013; Pires et al., 2020; Liu et al., 2025). Although these studies provide valuable insight into the vulnerability of pipelines, they often overlook point-type facilities such as wells, storage tanks, and pump stations that are equally essential for system functionality.

Research on point facilities has gradually expanded over the years. Chadha et al., (2008) reported spike-like water level fluctuations in Koyna bore wells triggered by the 2004 Sumatra earthquake, highlighting the sensitivity of wellheads to distant seismic waves. Such observations empirically document well response to teleseismic waves but provide no fragility functions for structural loss estimation.

Similarly, Huang et al., (2015) observed analogous responses in Beijing's well network during the 2001 Kunlun event, suggesting that even modest ground motions can perturb groundwater levels. Their findings further support the applicability of such responses; however, they still lack fragility functions for structural damage estimation.

Amin et al., (2021) examined the seismic vulnerability of reinforced concrete-supported tanks and introduced a response reduction coefficient that accounts for a wide range of tank geometries. Their work provides analytical fragility for modern code-compliant tanks but excludes aging and degradation. Subsequent experimental and numerical studies (Uma et al., 2021; Chitte et al., 2022; Tavasoli et al., 2022) confirmed that tank performance is highly sensitive to water height, foundation type, and Soil-Structure Interaction[4]. However, these studies primarily focus on newly designed code-based structures, conceptual R-factor analysis, or specific tank typologies, and do not address aging infrastructure.

Rimal et al., (2023) further refined fragility curves for aging elevated tanks by incorporating mat

[1] Japan International Cooperation Agency (JICA)

[2] Peak Ground Acceleration (PGA)

[3] Spectral Acceleration (SA)

[4] Soil–Structure Interaction (SSI)

foundations and SSI effects, revealing that older tanks often exhibit dramatically higher collapse probabilities than newer, code-compliant structures. Their study directly addresses aging elevated tanks; however, the fragilities require local calibration.

Eskandari et al., (2024) employed graph theory to capture interdependencies between water network facilities and other critical infrastructures. However, their study does not account for aging, outdated design codes, or anchorage deficiencies in vulnerability assessments.

More recently, Hou et al., (2026) introduced a novel framework for assessing the seismic resilience of water treatment plants, accounting for both component damage and interdependencies through a state-tree model to better represent dynamic functionality and recovery following earthquakes.

Despite extensive research on lifeline seismic risk, Iran's active regions still lack component-level assessments that consider outdated design codes, inconsistent anchorage, and decades of degradation. This study addresses this gap by providing three distinct contributions: (1) the first probabilistic seismic loss estimation for Kashan's water infrastructure with a detailed inventory of individual components; (2) integration of design-code and degradation modification factors; and (3) a sensitivity analysis to quantify the influence of degradation factors on damage estimates. To achieve this, the study compiles the necessary component data for wells, storage tanks, and pumps stations including construction dates, anchorage conditions, and observed deterioration. It then applies HAZUS (FEMA, 2022) empirical fragility functions to wells, on-ground tanks, and pump stations, while using analytically derived fragility curves for elevated concrete tanks lacking empirical data.

Finally, it adjusts fragility parameters using two correction factors, one reflecting the seismic code in force at construction and another representing degradation over service life. Loss scenarios are evaluated for a Design-Basis Earthquake[1] and a Maximum Considered Earthquake[2]. The combination of modified fragilities and ground motion intensity measures yields damage probability distributions across five damage states[3]. The resulting risk maps identify spatial clusters of high collapse probability, enabling prioritized mitigation actions.

2. Seismic hazard assessment

Kashan is situated within a highly seismically active zone in Central Iran, largely influenced by the Kashan fault (Jamali et al., 2011). This region of Central Iran exhibits a complex seismicity, characterized by the potential for large-magnitude earthquakes and seismic gaps along numerous Quaternary faults (Tabaei et al., 2016). The area has a documented history of seismic activity, including both historical events and more recent instrumental recordings (Melville and Ambraseys, 2005; Adib and Kianoush, 2025).

Fig. 1 illustrates the seismic epicenter map and the primary fault lines affecting Kashan and its surrounding environs.

This study utilizes probabilistic seismic hazard analysis from the Earthquake Model of the Middle East[4] project (Danciu et al., 2018; Şeşetyan et al., 2018), to estimate potential losses within Kashan's water system. The EMME seismic source model incorporates both active and inactive geological faults. To account for local site effects, surface ground motion amplitudes were estimated using Borcherdt's amplification factors (Borcherdt, 1994), based on soil classifications outlined in the Iranian seismic design code (BHRC, 2014). Due to the lack of a detailed soil classification map, the predominant soil type III (characterized by the top 30 m shear wave velocity of 175–375 m/s) was selected based on expert judgment and analysis of available geotechnical data from the study area (Municipality of Kashan, 2015; Kashan Water and Wastewater Engineering Company, 2017; Renovation Administration of Isfahan Province Schools, 2023).

Fig. 2 presents PGA values for 475-year (DBE) and 2475-year (MCE) return periods at bedrock level in Kashan. The resulting PGA hazard maps are broadly consistent with findings from other research (Tehran Padir Consultant Engineering, 2012).

3. Water system components at seismic risk

Fig. 3 illustrates the spatial distribution of components within Kashan's water system. The system's main elements are categorized as either pipe networks or point components. The point components encompass water wells, storage tanks, and pump stations, each consisting of several subcomponents. Details regarding component characteristics, including geographical location, classification, and construction year, were gathered through field surveys and data provided by the Kashan Water and Wastewater Engineering Company (personal communication).

Kashan's total potable water supply is approximately 1,320 L/s, primarily sourced from groundwater (83.3%) and surface water (16.7%). Table 1 provides details on the water wells, each with a capacity ranging from 4 to 35 L/s. These wells typically consist of a riser pipe, well casing, water pump, and a building that houses the well equipment.

[1] Design-Basis Earthquake (DBE)

[2] Maximum Considered Earthquake (MCE)

[3] Damage States (DS)

[4] Earthquake Model of the Middle East (EMME)

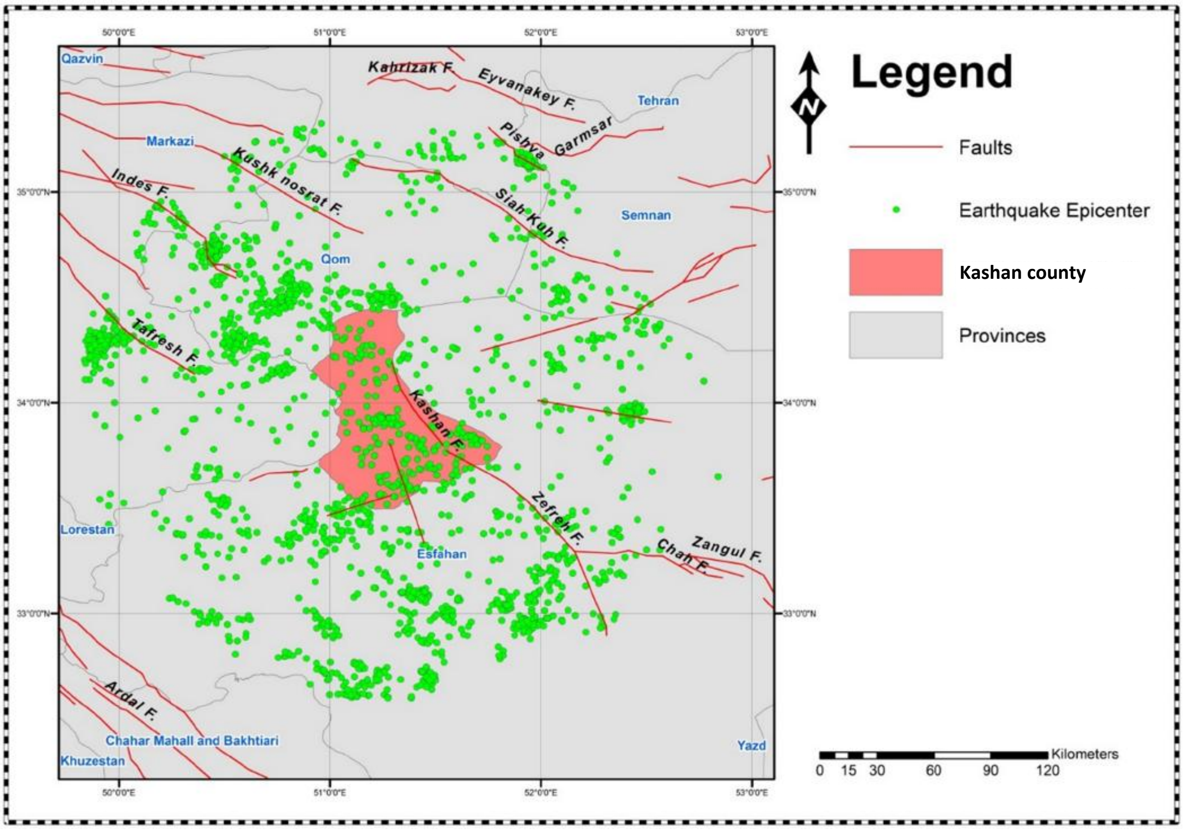

Fig. 1. Main faults and earthquake epicenters in the Kashan region (Adib and Kianoush, 2025)

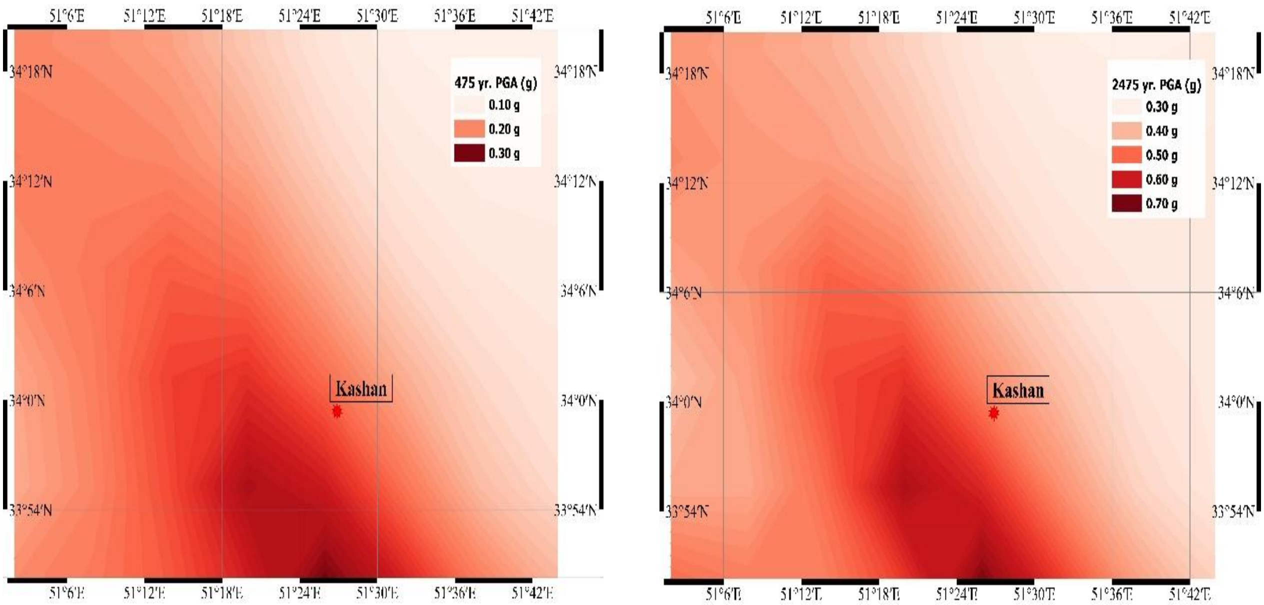

a) b)

Fig. 2. PGA at bedrock for Kashan and surrounding area: (a) 475-year return period, (b) 2475-year return period (Tahghighi and Ghafoori, 2023)

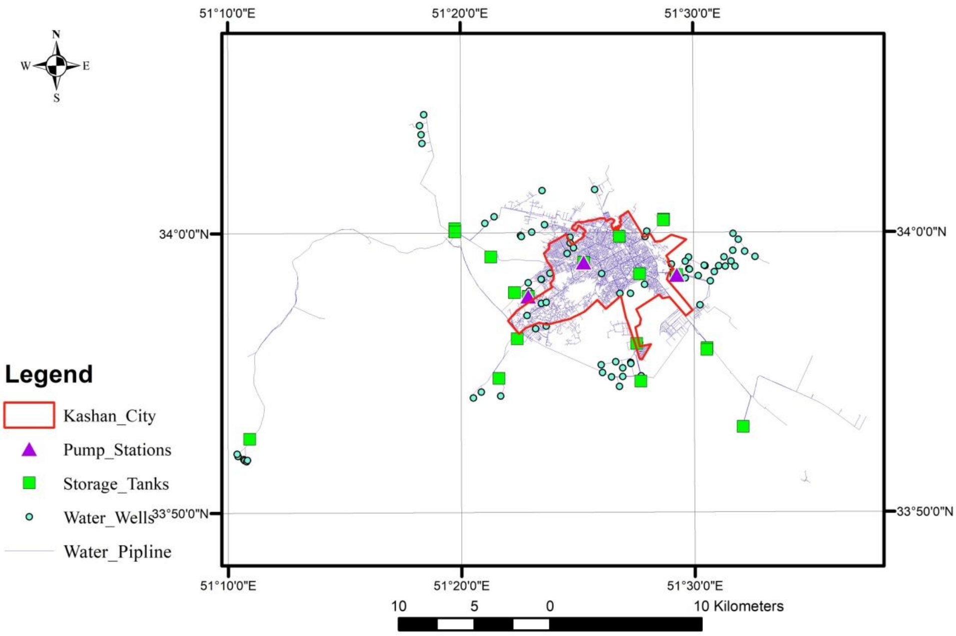

Fig. 3. Distribution of water system components in Kashan

Table 1. Characteristics of water supply wells

No.	Well number	Discharge (L/s)	Depth (m)	Electricity demand (kW)	Construction year	No.	Well number	Discharge (L/s)	Depth (m)	Electricity demand (kW)	Construction year
1	2	13	180	50	1966	25	26-2	0	40	-	2008
2	3	6	180	85	1995	26	27	10	170	50	1987
3	2	11	150	50	1995	27	28	9	170	50	1988
4	4	Off	-	-	1995	28	29-2	5	-	-	2010
5	5	13	160	50	2003	29	30	30	210	45	2006
6	7	12	150	50	1968	30	31	9	180	-	2012
7	8	22	150	45	1963	31	31-2	13	180	-	2012
8	11	8	200	60	2003	32	32	9	-	-	2006
9	12	9	180	-	2004	33	33	9	180	-	1983
10	13	off	-	-	2011	34	34	9	180	-	1990
11	13-2	17	170	80	2011	35	35	6	180	-	1990
12	14	5	-	-	2007	36	36	14	180	-	1989
13	15	25	150	-	2018	37	37	11	200	130	1989
14	16-2	11	170	60	2011	38	38	4	180	-	1989
15	17	12	-	50	2006	39	39	9	180	-	2006
16	18	12	170	50	1970	40	40	15	160	-	1991
17	19	16	150	60	1970	41	41	10	180	45	1992
18	21	8	150	55	2010	42	42	off	-	-	1992
19	21-2	8	150	55	2009	43	42-2	10	180	90	2004
20	22	19	250	100	2006	44	43	19	200	120	2010
21	23	9	150	60	2015	45	43-2	19	200	120	2010
22	23-2	9	150	60	2015	46	44	24	180	50	1993
23	24	17	150	55	1980	47	45	23	-	65	2009
24	25	25	150	85	1982	48	46	12	180	50	2008

Con. Table 1. Characteristics of water supply wells

No.	Well number	Discharge (L/s)	Depth (m)	Electricity demand (kW)	Construction year	No.	Well number	Discharge (L/s)	Depth (m)	Electricity demand (kW)	Construction year
49	46-2	12	180	50	2008	67	59	24	-	-	2009
50	47	15	200	80	1991	68	71	9	180	75	1994
51	48	15	-	-	2010	69	73	7	170	40	1981
52	49	15	-	-	2015	70	74	10	200	60	2006
53	50	7	150	100	2011	71	75	5	200	52	2006
54	50-2	7	150	100	2011	72	76	10	180	40	1992
55	51	8	250	80	2012	73	77	5	200	85	2006
56	51-2	8	250	80	2012	74	81	28	250	124	1997
57	52	8	180	100	2012	75	82	34	250	95	1992
58	52-2	8	180	100	2014	76	83	35	250	95	1993
59	53	13	250	85	2008	77	84	27	250	95	1997
60	53-2	13	250	85	2008	78	85	24	250	85	1996
61	54	19	250	80	1994	79	86	21	250	85	1996
62	55	7	250	80	2014	80	95	off	-	-	2018
63	55-2	7	250	85	2014	81	92	10	200	-	2018
64	56	12	180	75	2001	82	94	18	200	-	2018
65	57	22	200	45	2001	83	96	13	202	-	2018
66	58	24	200	125	2006	84	98	29	192	-	2018

Kashan's water storage system comprises 25 tanks with a combined capacity of 106,050 m³, consisting of 20 relatively modern, on-ground concrete tanks (totaling 101,000 m³) and five older, elevated tanks (with a capacity of 5,050 m³). It is worth noting that two of the elevated tanks, representing a total capacity of 1,750 m³, are currently out of service. Table 2 provides a detailed breakdown of the water storage tank characteristics.

Four water pump stations are strategically located to supply water to elevated areas in southern and southwestern Kashan, and to facilitate transfers between reservoirs. Table 3 outlines the characteristics of these pump stations, all classified as small-sized (with a capacity of less than 440 L/s) (FEMA, 2022). Each station includes electrical equipment, at least one pump, a station building, and, in some instances, backup power systems. Identifying these critical components provides the foundation for the fragility-based vulnerability modeling discussed in the next section.

4. Methodology

Fig. 4 presents a flowchart summarizing the proposed methodology through seven sequential steps: (1) field data collection and component identification (Section 3); (2) seismic hazard definition (Section 2); (3) fragility selection and modification factor application (Sections 4.1 and 4.2); (4) damage probability and sensitivity analysis (Sections 4.3 and 4.4); (5) validation via alternative methods (Section 5.1); (6) loss estimation and risk mapping (Section 5); and (7) mitigation prioritization (Section 6). Each step is cross-referenced to the corresponding section.

4.1. Fragility models

Earthquakes increase structural vulnerability through ground failures like liquefaction, landslides, and faulting, as well as through ground shaking. Fragility models are valuable tools for evaluating earthquake risk and informing the development of effective crisis management strategies. This section focuses on seismic fragility models specifically for point components within the water system. Considering the minimal potential for liquefaction and landslides in the study area (Tehran Padir Consultant Engineering, 2012), the possibility of damage from these geohazards was not included in the analysis. Furthermore, due to a lack of data regarding facility proximity to faults and resulting deformation patterns, damage caused by faulting was also excluded. Consequently, the point components examined in this study are primarily vulnerable to ground motion intensity measures, such as PGA.

Vulnerability levels for each system component are categorized into five DS: None (undamaged), Slight (minor damage), Moderate (considerable damage), Extensive (severe damage), and Complete (collapse). These DS are detailed in the HAZUS methodology (FEMA, 2022). The HAZUS risk model has been widely adopted by researchers to assess the seismic vulnerability of lifeline systems globally (e.g., Eskandari et al., 2020; Pavel et al., 2021; Wu et al., 2023).

Table 2. Characteristics of water storage tanks

No.	Name	Capacity (m^3)	Classification	Construction year
1	Ravand#1	1000	On-ground concrete	1983
2	Facilities#4	2000	On-ground concrete	1995
3	Ravand#2	2000	On-ground concrete	1995
4	Facilities#1	1500	On-ground concrete	1980
5	Ravand#3	500	On-ground concrete	1987
6	Facilities#6	10000	On-ground concrete	2008
7	Facilities#6	1000	On-ground concrete	1999
8	Facilities#6	2000	On-ground concrete	2001
9	Facilities#10	4000	On-ground concrete	2011
10	Facilities#2	6000	On-ground steel	1979
11	Facilities#3	10000	On-ground concrete	1985
12	Facilities#4	4000	On-ground concrete	1996
13	Facilities#4	2000	On-ground concrete	1996
14	Facilities#5	4000	On-ground concrete	1995
15	Facilities#5	1000	On-ground concrete	1992
16	Facilities#8	10000	On-ground concrete	2010
17	Facilities#8	10000	On-ground concrete	2020
18	Facilities#RF2	10000	On-ground concrete	2010
19	Facilities#RS2	15000	On-ground concrete	2010
20	Facilities#RS3	5000	On-ground concrete	2006
21	Facilities#1	300	Elevated steel	1962
22	Facilities#1	1500	Elevated concrete	1957
23	22 Bahman St.	1500	Elevated concrete	1957
24	Natanz St.	1500	Elevated concrete	1957
25	Big Finn	250	Elevated steel	1961

Table 3. Characteristics of water pump stations

No.	Station name	Capacity (L/s)	Destination	Number of pumps	Network power (kW)	Emergency power (kW)	Construction year
1	Facilities#1	100	Elevated tank	6	140	175	1995
2	Facilities#2	70	Network	2	50	50	2007
3	Facilities#4	140	Facilities#6	2	120	-	1997
		200	Network	4	200	-	1997
4	Moratab facilities	35	Sanaye tank#2000	1	100	-	2007

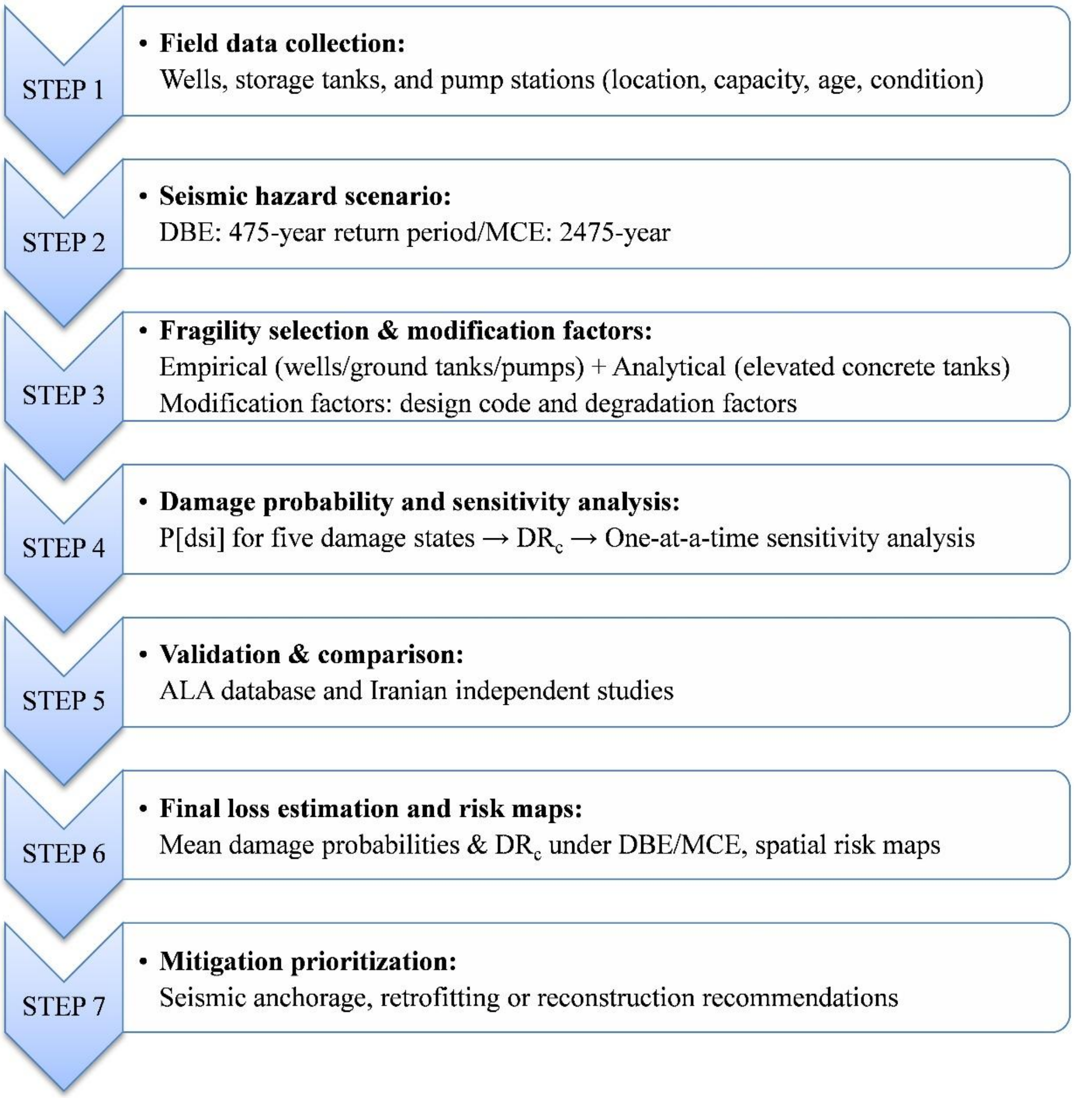

Fig. 4. Flowchart of the proposed seismic loss estimation methodology

Typically, the accuracy of an empirical fragility model is evaluated by comparing its predictions with field observations from past earthquakes. However, the limited occurrence of large earthquakes near urban areas has resulted in a scarcity of regions that can be accurately assessed through earthquake modeling. Consequently, analytical and expert-based techniques are often employed to develop fragility curves. Analytical fragility curves are derived from structural seismic responses using advanced analysis models, such as incremental dynamic analysis (Alam et al., 2023). A primary limitation of analytical methods is the substantial computational resources required to generate fragility functions.

Lognormal distributions are generally employed to represent fragility functions for water system components, quantifying the likelihood that a particular damage state will be reached or exceeded at a given intensity measure level. For more complex assets, these functions can be assembled through fault-tree analysis that combines the fragility curves of individual subcomponents (Porter and Ramer, 2012; Terzic and Villanueva, 2021). Each fragility curve is defined by a median intensity (μ) and a dispersion parameter (β) that describes the uncertainty in the estimate of the median value, the latter being the logarithmic standard deviation of the intensity measure. Consequently, the vulnerability model expresses the probability of being in or exceeding each discrete damage state (ds_i) via the cumulative distribution shown in Equation 1

$$P(DS \geq ds_i \mid IM = x) = \Phi\left[\frac{1}{\beta}\ln\left(\frac{x}{\mu}\right)\right] \quad (1)$$

Table 4. PGA fragility functions for water system components (FEMA, 2022)

Component	Damage state							
	Slight		Moderate		Extensive		Complete	
	Median(g)	β	Median(g)	β	Median(g)	β	Median(g)	β
Water well	0.15	0.75	0.36	0.65	0.72	0.65	1.50	0.80
On-ground concrete tank	0.25	0.55	0.52	0.70	0.85	0.60	1.64	0.70
On-ground steel tank	0.15	0.70	0.35	0.75	0.68	0.75	0.95	0.70
Elevated steel tank	0.18	0.50	0.55	0.50	1.15	0.60	1.50	0.60
Pump station, small	0.15	0.70	0.36	0.65	0.66	0.65	1.50	0.80

Table 5. Spectral displacement fragility functions for elevated concrete tanks

Component	Damage state	Median (mm)	Dispersion (β)
Elevated concrete tank	Slight	19	0.50
	Moderate	33	0.53
	Extensive	59	0.60
	Complete	125	0.69

Where
x represents the seismic intensity measure such as PGA. The dispersion parameter, β, is expressed in terms of randomness (β_r) and uncertainty (β_u) components (Kennedy et al., 1980). To account for uncertainty, the dispersion parameters for both the earthquake hazard and the component are combined into a total dispersion estimate using Equation 2, which is used throughout the evaluation

$$\beta_{total} = \sqrt{\beta_u^2 + \beta_r^2} \quad (2)$$

The probabilities of being in various DS are then calculated using equations 3 to 7 following the HAZUS methodology (FEMA, 2022)

$$P(DS = None) = 1 - P(DS \geq Slight) \quad (3)$$

$$P(DS = Slight) = P(DS \geq Slight) - P(DS \geq Moderate) \quad (4)$$

$$P(DS = Moderate) = P(DS \geq Moderate) - P(DS \geq Extensive) \quad (5)$$

$$P(DS = Extensive) = P(DS \geq Extensive) - P(DS \geq Complete) \quad (6)$$

$$P(DS = Complete) = P(DS \geq Collapse) \quad (7)$$

The HAZUS methodology assumes general seismic anchorage for equipment and subcomponents within water wells. It also provides fragility functions for both on-ground (concrete or steel) and elevated steel tanks. These fragility curves are applicable to liquid storage tanks maintaining at least 80% capacity during seismic events. For on-ground tanks, unanchored fragility functions were utilized, reflecting the common construction practice observed in the study area. For elevated concrete tanks lacking empirical fragility relationships that align with the defined DS, analytical models developed by Amin et al., (2021), accounting for full-reservoir conditions, were implemented. Furthermore, pump stations were categorized based on whether their subcomponents (such as mechanical and electrical equipment) were anchored or unanchored. Based on visual site assessments, the subcomponents were determined to be unanchored.

Table 4 summarizes the median values and dispersions of the empirical fragility functions for various DS associated with water wells, unanchored on-ground tanks, elevated steel tanks, and unanchored pump stations. Fragility parameters for anchored components can be found in the HAZUS methodology. While Table 5 presents the median and dispersion values for the analytical fragility functions of elevated concrete tanks, expressed in terms of spectral displacement, S_d (mm). The spectral displacement for each location was determined by converting the spectral acceleration S_a (g) for a specific period T (s) using Equation 8

$$S_d = 248 \times S_a \times T^2 \quad (8)$$

Fig. 5 illustrates the analytical fragility curves for elevated concrete tanks, which have been modified to account for SSI effects at higher DS, following the analysis presented by Rimal et al., (2023).

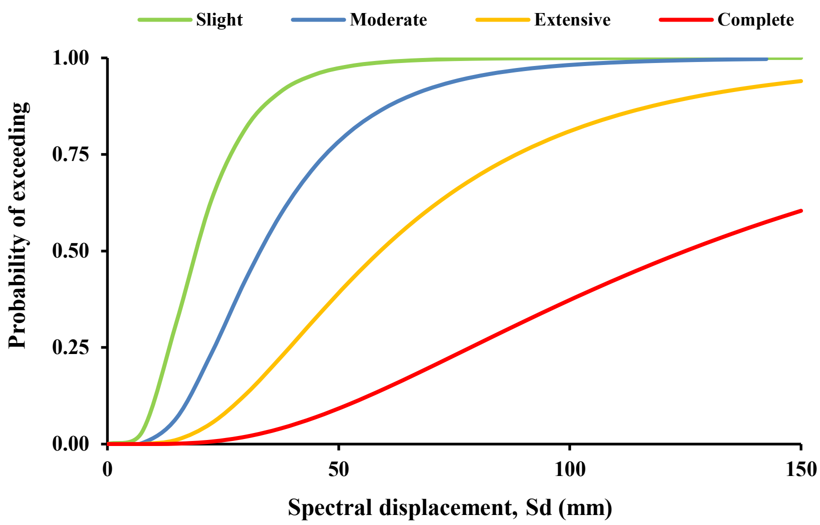

Fig. 5. Analytical fragility curves for elevated concrete tanks (full reservoir, 1500 m[3] capacity) (Amin et al., 2021)

4.2. Modification factors

Iran's first national seismic regulations were established by the Plan and Budget Organization in 1964 (Moinfar et al., 2012), in response to the devastating 1962 Buin-Zahra earthquake (M_w 7.2). The importance of this code became particularly apparent following the destructive 1990 Rudbar-Manjil earthquake (Mw 7.3), leading to its broader implementation in structural design. To account for the potential five-year discrepancy between design standards and actual construction practices, a fragility modification factor was applied, following the methodology outlined in the JICA report (JICA, 2006), to address variations in seismic design conditions. Consequently, the water system components were categorized by their construction period, with corresponding fragility modification factors reflecting the applicable seismic design code: 1.0 (post-1995, high-code), 1.5 (1969-1995, low-code), and 2.0 (pre-1969, pre-code), as summarized in Table 6.

Component degradation was assessed through a combination of field surveys and a review of existing literature (JICA, 2006; Fakhimi and Rahemi, 2014). Observed deterioration included cracking, inadequate concrete cover over reinforcement, concrete spalling, steel corrosion, reduced structural strength, settlement, and deformation. To quantify the impact of progressive aging, degradation-induced fragility modification factors were established: 1.0 (representing minor degradation), 1.5 (moderate degradation), and 2.0 (severe degradation), as summarized in Table 7.

4.3. Compounded damage ratio[1]

To estimate expected direct physical losses, the DRc is introduced as a single damage parameter. The DR_c index, defined using Equation 9, probabilistically combines the damage state probabilities P[dsi] (calculated from Equations 3 to 7) with corresponding Damage Ratios[2] to represent the most probable damage state of a component under a given seismic hazard

$$DR_c = \sum_{i=2}^{5} DR_i \times P\left[ds_i\right] \qquad (9)$$

Where

DR_i values are adopted from Table 8 based on the HAZUS Inventory Technical Manual (FEMA, 2022). No losses are associated with damage state 1 (None); therefore, the summation is from i = 2 to 5. DR_c ranges from 0 to 1 and is further used in Section 5 to compare expected hydraulic losses across different seismic scenarios and anchorage conditions.

4.4. Sensitivity analysis of fragility modification factors

To address the uncertainty in the selected fragility modification factors, i.e. degradation and design factors (1.0, 1.5, 2.0), a one-at-a-time sensitivity analysis was performed following the approach of Gopisetti et al., (2021). The modification factor for each component category was varied independently from -20% to +20% of the baseline value (in steps of 0.1), while all other parameters were held constant. The damage probability was recomputed for each variation. To quantify the sensitivity, the Normalized Sensitivity Index[3] is defined

[1] Compounded Damage Ratio (DR_c)

[2] Damage Ratios (DR_i)

[3] Normalized Sensitivity Index (NSI)

Table 6. Seismic design fragility modification factors (JICA, 2006)

Risk factor	Scope	Seismic design level	Design factor
Construction year	Post-1995	High-code	1.0
	1969-1995	Low-code	1.5
	Pre-1969	Pre-code	2.0

Table 7. Degradation fragility modification factors (JICA, 2006)

Risk factor	Scope	Degradation factor
Degradation degree	Minor	1.0
	Moderate	1.5
	Severe	2.0

Table 8. DR_i for water system components (FEMA, 2022)

Component	Damage state			
	Slight	Moderate	Extensive	Complete
Wells and pump station	0.05	0.38	0.80	1.00
Storage tank	0.20	0.40	0.80	1.00

as the relative change in DR_c divided by the relative change in the input factor, as shown in Equation 10

$$NSI = \frac{\Delta DR_c}{\Delta F} \frac{F_{base}}{DR_{c,base}} \tag{10}$$

Where

ΔDR_c is the change in the compounded damage ratio, $DR_{c,base}$ is its baseline value, ΔF is the change in the modification factor, and F_{base} is its baseline value. This index provides a practical interpretation of sensitivity by relating a given percentage change in an input parameter to the corresponding percentage change in the output relative to its baseline value. The selected modification factors are based on observed deterioration from field surveys and Iran's seismic design code history, providing locally calibrated adjustments to the fragility functions (see also Section 4.2). The results of this analysis are presented in Section 5.

5. Earthquake loss estimation

Following the methodology outlined in Section 4 and summarized in Fig. 4, this section presents loss estimates for wells, storage tanks, and pump stations under DBE and MCE scenarios, considering design levels, degradation, and anchorage. Results include component-level losses, sensitivity analysis, hydraulic loss comparison, and validation against previous studies and observed data.

Fig. 6 shows the spatial distribution of loss estimates for water wells across various DS. Under DBE ground motions, the probabilities of experiencing slight, moderate, extensive, and complete damage increase by 47%, 32%, 8%, and 3%, respectively. For MCE scenarios, these probabilities increase to 42%, 41%, 20%, and 8% for the same DS. This comparative analysis reveals that higher-intensity shaking (MCE) significantly increases the likelihood of moderate, extensive, and complete DS. Conversely, the probabilities of no damage and slight damage are higher under DBE conditions.

As previously outlined, empirical fragility functions were employed to evaluate seismic damage for the majority of storage tanks, with the exception of three elevated concrete tanks #22-24 detailed in Table 2. These functions were adjusted for design and degradation influences using correction factors presented in Tables 6 and 7.

For the three circular tanks featuring concrete cylindrical shafts, FEM-based seismic fragility functions, accounting for SSI effects, were adapted from existing research (Amin et al., 2021; Rimal et al., 2023). Fundamental periods were determined via a single-degree-of-freedom model, resulting in periods of 0.40 s, 0.51 s, and 0.25 s for elevated tanks #22-24, respectively, under full reservoir conditions.

Fig. 7-a illustrates the distribution of expected losses for both on-ground and elevated reservoirs under DBE conditions. Aging structures demonstrate high vulnerability; specifically, on-ground steel Tank #10 exhibits a 31% probability of extensive damage and a 20% risk of collapse, while flexible-based elevated concrete Tank #23 shows a 57% probability of extensive damage and a 12% probability of complete damage.

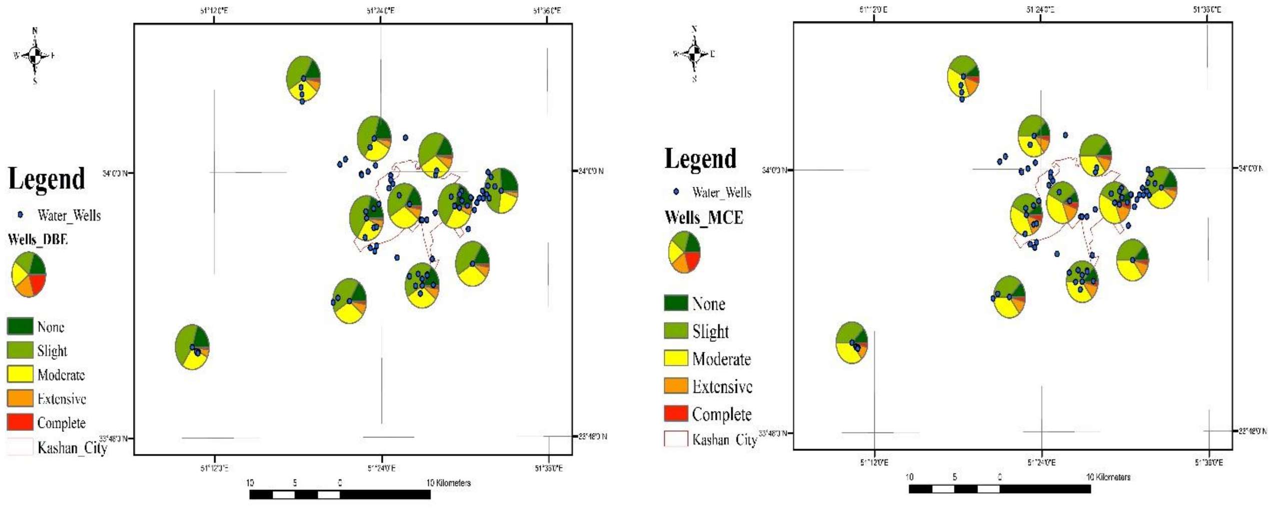

a) b)

Fig. 6. Loss estimation map of water wells: (a) DBE, (b) MCE

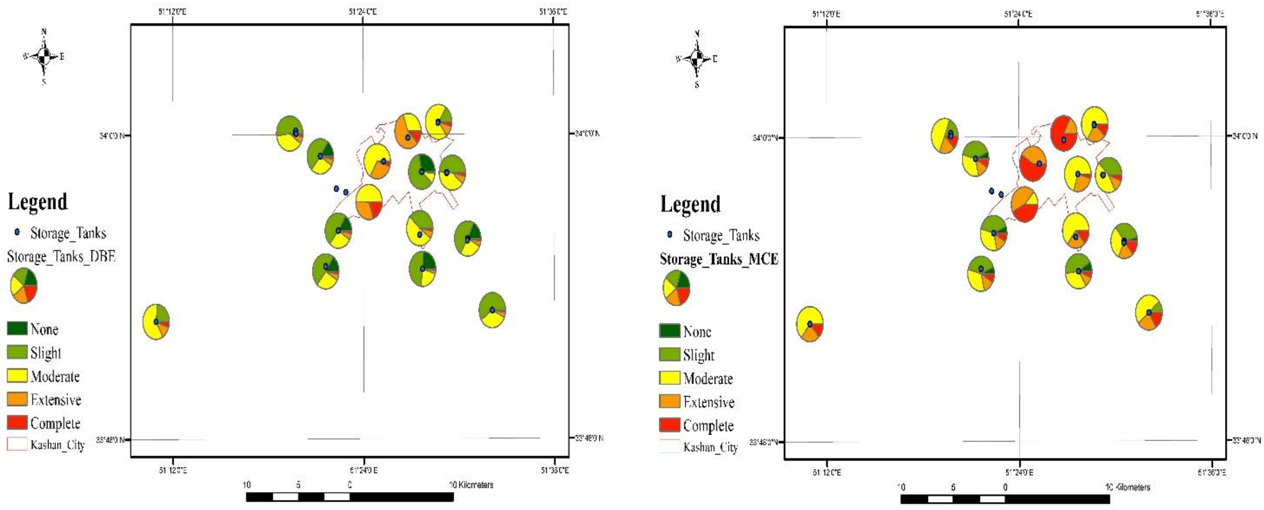

a) b)

Fig. 7. Loss estimation map of storage tanks: (a) DBE, (b) MCE

Fig. 7-b presents the loss analysis map for storage reservoirs subjected to MCE ground motions, revealing increased vulnerability for elevated reservoirs. Notably, Tanks #10 (43%) and #23 (83%) display the highest collapse probabilities, signifying critical failure risks during MCE events. Comparative analysis indicates that elevated tanks exhibit higher mean probabilities for severe DS compared to on-ground tanks, likely due to the combined influence of structural aging and SSI. Moreover, MCE conditions lead to a significant increase in structural damage probabilities for moderate, extensive, and complete states relative to DBE levels. Conversely, DBE scenarios result in higher probabilities of slight damage.

Fig. 8 shows the spatial distribution of seismic risks for pump stations under both DBE and MCE ground motions. As previously noted, the empirical fragility functions were modified to account for design and degradation effects, utilizing the adjustment factors in Tables 6 and 7. A comparison of the results indicates that MCE scenarios result in higher mean damage probabilities than DBE conditions for severe states, often causing prolonged service disruptions. In contrast, DBE produces greater probabilities of slight to moderate damage compared to MCE, affecting operational efficiency.

Table 9 compares the DR_c and mean damage probabilities for all water system point components under two distinct seismic hazard levels. As shown, storage tanks exhibit the highest collapse potential and functional loss probabilities among all component types. Under the MCE scenario, elevated tanks show the

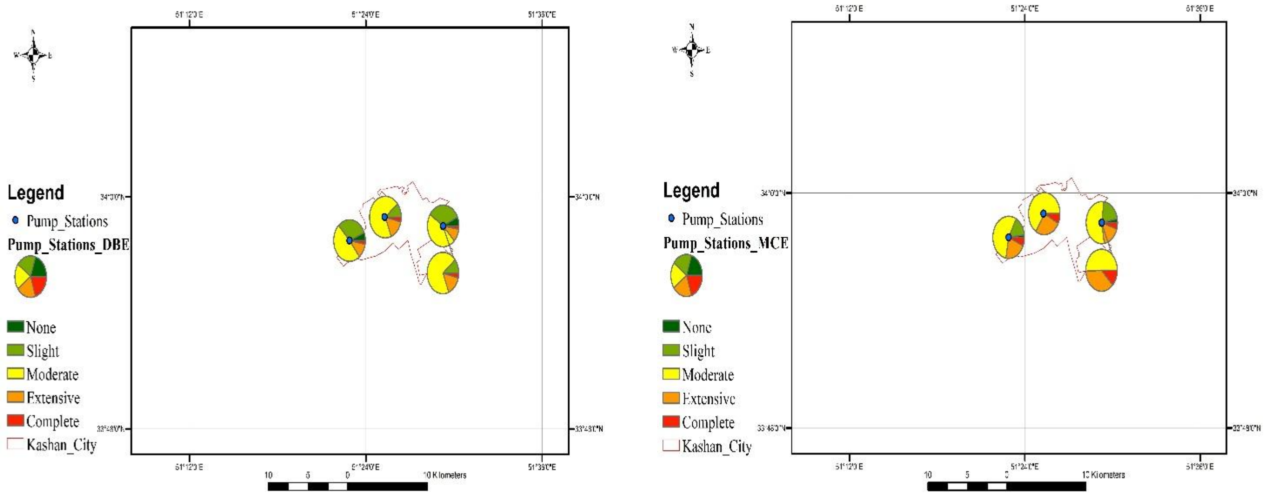

a) b)

Fig. 8. Loss estimation map of pump stations: (a) DBE, (b) MCE

Table 9. Mean damage parameters (%) for water system components under DBE and MCE conditions

Component	Damage state										DRc	
	None		Slight		Moderate		Extensive		Complete			
	DBE	MCE	DBE	MCE	DBE	MCE	DBE	MCE	DBE	MCE	DBE	MCE
Water well	18.74	11.39	43.64	36.40	29.16	36.32	6.35	11.66	2.10	4.22	20.4	29.2
On-ground tank	5.68	1.81	42.20	18.81	40.01	42.53	8.10	21.72	4.00	15.13	34.9	53.3
Elevated tank	5.68	0.00	28.03	0.00	43.39	46.01	18.91	21.89	3.99	32.10	42.1	68.0
Pump station	3.26	1.21	21.71	8.83	58.70	56.54	13.05	25.48	3.28	7.94	37.1	50.2

highest mean complete damage probability (32.1%) and the highest DR_c (68.0%), confirming their critical vulnerability under severe ground motions. On-ground tanks follow with a complete damage probability of 15.1% and DR_c of 53.3%, while pump stations show lower values (7.9% and 50.2%, respectively).

Water wells exhibit the lowest vulnerability, with a mean complete damage probability of approximately 4% and a DRc of 29.2% under MCE. Under DBE conditions, elevated tanks again show the highest DR_c (42.1%) and the highest slight damage probability (60.0%), while on-ground tanks show a complete damage probability of 4.0% and water wells show the lowest DR_c (20.4%). These results highlight the significant influence of seismic intensity on the expected performance of water system components, with elevated tanks consistently showing the highest vulnerability across all DS.

The damage analyses were carried out for both anchored and unanchored on-ground tanks and pump stations, underscoring the importance of seismic anchorage in loss assessments. Fig. 9 presents a comparison of mean damage probabilities for water system components under anchored versus unanchored conditions for both DBE and MCE demands. The results reveal that elevated storage tanks and unanchored on-ground tanks are the most susceptible to collapse and functional loss among all component types.

Table 10 further quantifies these findings by comparing mean damage parameters for anchored versus unanchored conditions. The results demonstrate that unanchored on-ground tanks under MCE show substantially higher DR_c (53.3%) and complete damage probability (15.1%) compared to anchored conditions (40.3% and 5.5%, respectively). Similarly, unanchored pump stations under MCE exhibit higher DR_c (50.2%) compared to anchored ones (45.7%). The most pronounced differences between anchored and unanchored conditions are observed for on-ground tanks under MCE, where the complete damage probability increases by approximately threefold in the absence of anchorage, and for pump stations under DBE, where the moderate damage probability increases from 36.7% (anchored) to 58.7% (unanchored). Consistent with the visual comparison in Fig. 9, these findings confirm that proper seismic anchorage effectively reduces potential losses in these facilities. Additional risk mitigation strategies exist, including retrofitting measures that can

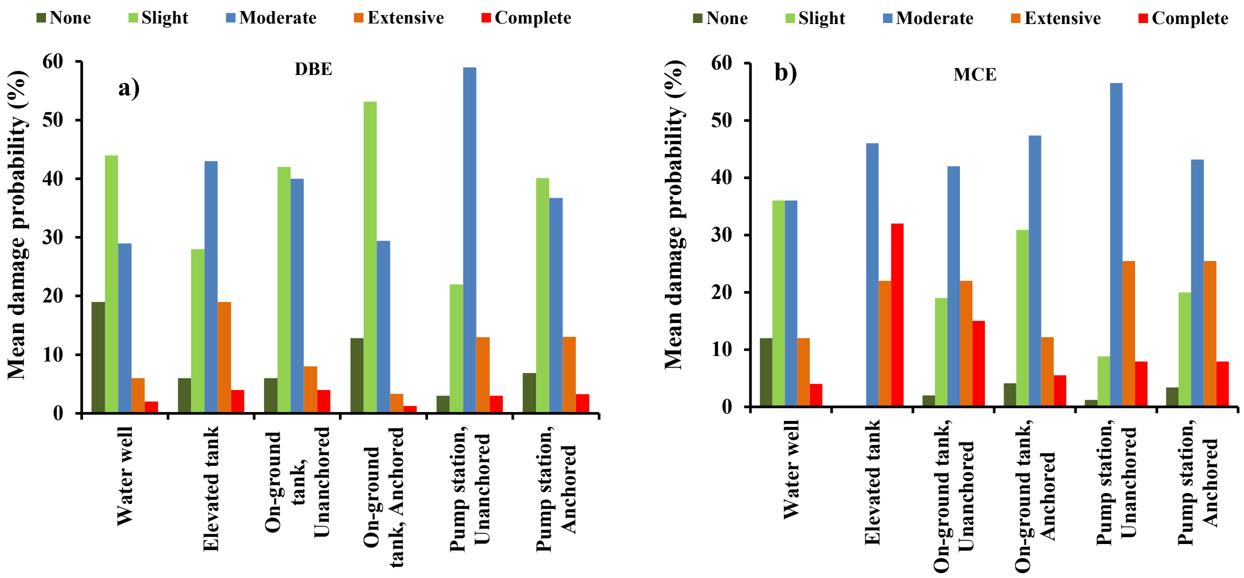

Fig. 9. Mean damage probabilities for anchored vs. unanchored components under (a) DBE and (b) MCE

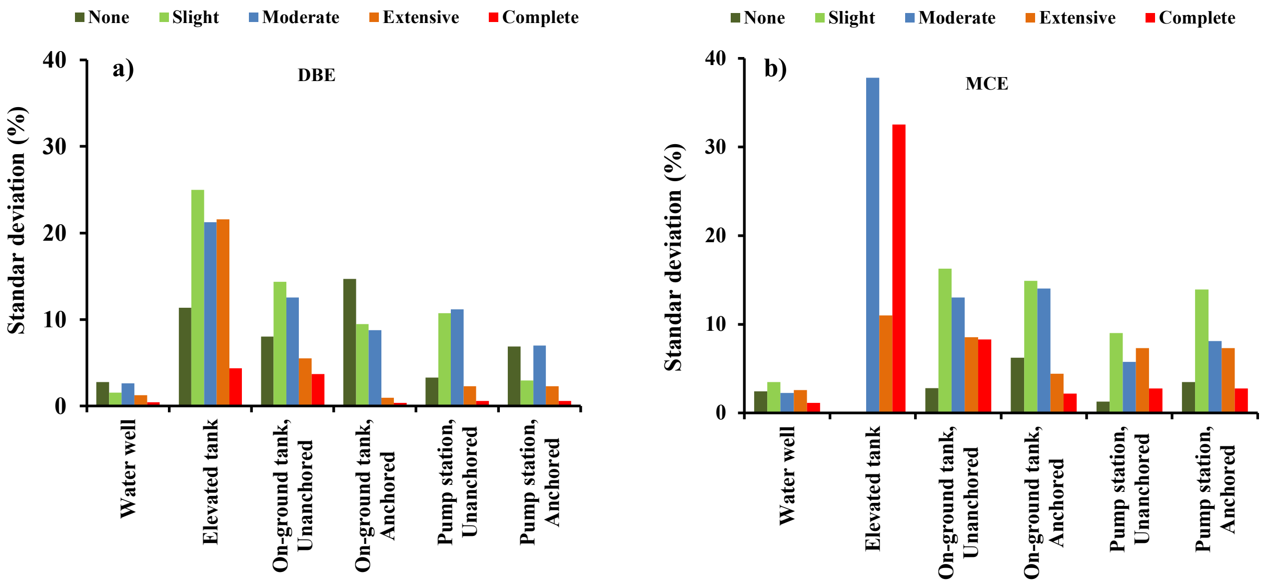

Fig. 10. Standard deviations of damage probabilities for anchored vs. unanchored components under (a) DBE and (b) MCE

Table 10. Mean damage parameters (%) for unanchored and anchored components

Component	Earthquake scenario	Damage state										DR_c	
		None		Slight		Moderate		Extensive		Complete			
		Unanch.	Anch.	Unanch.	Anch.	Unanch.	Anch.	Unanch.	Anch.	Unanch.	Anch.	Unanch.	Anch.
On-ground tank	DBE	5.68	12.84	42.20	53.15	40.01	29.42	8.10	3.33	4.00	1.27	34.9	26.3
	MCE	1.81	4.10	18.81	30.86	42.53	47.36	21.72	12.18	15.13	5.49	53.3	40.3
Pump station	DBE	3.26	6.86	21.71	40.10	58.70	36.70	13.05	13.05	3.28	3.28	37.1	29.7
	MCE	1.21	3.41	8.83	19.99	56.54	43.18	25.48	25.48	7.94	7.94	50.2	45.7

Table 11. NSI to fragility modification factors

Component	$DR_{c,base}$	Factor variation (%)	DR_c range (min-max)	DR_c variation (%)	NSI
Elevated tank	0.421	±20	0.383- 0.457	±9	0.43
On-ground tank	0.349	±20	0.305- 0.390	±12	0.60
Pump station	0.371	±20	0.302- 0.424	±18	0.88

Table 12. Compounded DR_i (%) for all component types

Component	Condition	W/O factors		With factors		Fallah-Aliabadi et al., (2020)		Eskandari et al., (2024)	
		DBE	MCE	DBE	MCE	Scenario1	Scenario2	Independent loss	Dependent loss
Well	-	20.4	29.2	-	-	-	-	25.6	78.7
Elevated tank	-	20.3	39.7	42.1	68.0	28.5	36.2	13.0	97.0
On-ground tank	Unanch.	26.4	41.2	34.9	53.3	28.5	36.2	13.0	97.0
	Anch.	18.6	31.0	26.3	40.3	28.5	36.2	2.4	36.5
Pump station	Unanch.	30.6	44.0	37.1	50.2	-	-	22.1	100
	Anch.	24.4	37.4	29.7	45.7	-	-	4.6	77.9

Table 13. Expected hydraulic service loss under DBE and MCE scenarios

Component	Hydraulic parameter	Total capacity	DR_c (%)		Expected loss		Increase factor
			DBE	MCE	DBE	MCE	
Water well	Discharge (L/s)	1100	20.4	29.2	224	321	1.43
Elevated tank	Capacity (m^3)	5050	42.1	68.0	2319	3888	1.68
On-ground tank, Unanchored	Capacity (m^3)	101000	34.9	53.3	35279	50274	1.42
Pump station, Unanchored	Capacity (L/s)	545	37.1	50.2	223	308	1.38

further enhance resilience. However, for outdated wells, low-seismic standard installations, and pre-code storage tanks, reconstruction may be more economical than rehabilitation, as upgrade costs can exceed replacement expenses.

Fig. 10 shows the standard deviations of damage probabilities for the water system components, considering the seismic hazard levels of DBE and MCE. These standard deviations were calculated using the same dataset employed for determining the mean probabilities linked to specific DS. It is evident that the standard deviation for each damage state is lower than the corresponding mean probability. Overall, the highest standard deviations were found for elevated tanks and unanchored on-ground tanks.

The results of the sensitivity analysis indicate that pump stations exhibit the highest sensitivity, with DR_c ranging from 0.30 to 0.42 (a ±18% variation around the baseline estimate of 0.37). Ground-supported tanks show moderate sensitivity (±12%), while elevated tanks show lower sensitivity (±9%). For elevated tanks, the NSI is 0.43, meaning that a 10% increase in the modification factor leads to a 4.3% increase in damage ratio. This NSI, being less than 1.0, confirms that the results are not overly sensitive to the exact choice of modification factors. However, the higher sensitivity of pump stations suggests that future studies should prioritize more accurate degradation and design factor assessments for this component type. Table 11 summarizes the sensitivity analysis results for all component types under the DBE scenario, which is selected as the representative hazard level for this analysis.

5.1. Validation and comparison

Table 12 compares compounded DR_i for all components with two previous Iranian studies (Fallah-Aliabadi et al., 2020; Eskandari et al., 2024). The comparison shows reasonable agreement within ±10% for most components. Our method yields higher estimates than independent loss models (which ignore degradation and design factors) but lower than dependent loss models (which account for interdependencies), confirming that the degradation-factor approach provides a reasonable and balanced estimate.

According to ALA, (2001), elevated concrete tanks experience moderate damage (spalling at joints) at PGA

0.2–0.3g, with less than 5% collapse probability at PGA 0.4–0.5g. Our results show similar agreement: DR_c at DBE is 42% (with fragility modification factors) and 20% (without factors) at ~0.3g; DR_c at MCE is 68% (with factors) and 41% (without factors), corresponding to collapse risks of 32% and 6%, respectively, at ~0.4g.

Comparison with SRMLIFE (Pitilakis et al., 2014) shows that HAZUS estimates higher probabilities of slight-to-extensive damage, whereas SRMLIFE predicts substantially higher complete damage probabilities (Tahghighi and Ghafoori, 2023). For wells under MCE, the complete damage probability is 4% according to HAZUS, compared to 15% for SRMLIFE. SRMLIFE's distinction between low-code and high-code seismic design levels is particularly relevant for Kashan's wells, a significant number of which were constructed before 1995. Given the lack of local empirical validation, a hybrid conservative approach could be considered for risk management applications, adopting the higher damage probability from either model for each damage state, as proposed in the same reference.

While the above comparisons provide reasonable validation, full validation with empirical damage data remains a future need. Large earthquakes near Kashan are rare, and empirical data for direct calibration are currently unavailable. Subsequent research should prioritize the collection of post-earthquake damage data, site-effect microzonation, and fault-rupture considerations to further validate and refine the fragility functions used in this study.

5.2. Hydraulic service loss comparison

To further interpret the DR_c values in terms of expected hydraulic service loss, Table 13 presents the comparison of flow and volume losses across DBE and MCE scenarios. As shown in Table 13, elevated tanks exhibit the highest increase in expected service disruption under MCE conditions (1.68-times), followed by water wells (1.43-times), on-ground tanks (1.42-times), and pump stations (1.38-times). These results highlight the disproportionate vulnerability of elevated storage infrastructure under stronger ground motions, providing valuable insights for seismic risk mitigation planning in Kashan's water system.

Overall, the results indicate that elevated tanks are the most vulnerable components, while anchorage significantly reduces losses. The sensitivity analysis confirms that the results are robust to variations in modification factors, and the validation exercise supports the reliability of the proposed methodology.

6. Conclusions

This study presented a comparative seismic risk assessment for water system components, including wells, storage tanks (on-ground and elevated), and pump stations, in Kashan, Iran. The fragility analysis combined empirical HAZUS functions with analytical models, supported by field observations. Vulnerability assessments accounted for seismic anchorage, design code levels, and degradation effects through modification factors, yielding damage distributions across five states under DBE (475-year) and MCE (2475-year) scenarios. The DR_c was introduced as a single index to quantify expected physical and hydraulic losses. Key findings are as follows:

- Elevated tanks are the most vulnerable, with the highest DR_c (0.421 under DBE; 0.680 under MCE) and complete damage probability (4.0% under DBE; 32.1% under MCE).
- On-ground tanks and pump stations show moderate vulnerability, with DR_c values of 0.533 and 0.502 under MCE, respectively, while wells show the lowest DR_c (0.292).
- MCE scenarios cause severe damage and prolonged disruptions, while DBE scenarios result in slight to moderate damage, consequently impacting operational efficiency.
- Unanchored components show significantly higher losses; anchorage effectively reduces DR_c and damage probabilities.
- Elevated tanks experience the highest increase in service disruption under MCE (1.68-fold), followed by wells (1.43-fold), on-ground tanks (1.42-fold), and pump stations (1.38-fold).
- Mitigation should prioritize elevated tanks, followed by on-ground tanks, with anchorage, retrofitting, or reconstruction as key measures.

The findings support targeted risk mitigation strategies for Kashan and provide practical guidance for other seismically active regions. Future research should prioritize empirical validation using post-earthquake damage data, site-effect microzonation, and fault-rupture considerations to further refine fragility functions and improve loss estimation.

7. Acknowledgments

The authors gratefully acknowledge the financial support provided by the Kashan Water and Wastewater Engineering Company (Grant No. 401/36444). Special thanks are also extended to J. Parsa and M. Jafarzadeh for their invaluable cooperation. We also appreciate the anonymous reviewers for their insightful feedback, which helped enhance the quality of this work.

8. Funding

This study was funded by the Kashan Water and Wastewater Engineering Company (Grant No. 401/36444).

9. Conflict of interest

The authors declare that they have no conflict of interest.

References

ALA, 2001. *Seismic Fragility Formulation for Water System: Part 1- Guideline*. American Lifeline Alliance, ASCE. [Link]

Abbasnejadfard, M., Bastami, M. and Fallah, A., 2020. Investigation of anisotropic spatial correlations of intra-event residuals of multiple earthquake intensity measures using the latent dimensions method. *Geophysical Journal International*, 222(2), 1449-1469. https://doi.org/10.1093/gji/ggaa255.

Adib, A. and Kianoush, P., 2025. Enhanced seismic hazard assessment and risk zoning in the Kashan region, central Iran: insights from historical data and advanced modeling techniques. *Results in Earth Sciences*, 3, 100098. https://doi.org/10.1016/j.rines.2025.100098.

Alam, M. S., Simpson, B. G. and Barbosa, A. R., 2023. Fragility and recovery models for energy, water, and wastewater systems for seismic regional risk and resilience assessment: state-of-the-art review and database. *Natural Hazards Review*, 24(4), 04023036. https://doi.org/10.1061/NHREFO.NHENG-1661.

Amin, J., Gondaliya, K. and Mulchandani, C., 2021. Assessment of seismic collapse probability of RC shaft supported tank. *Structures*, 33, 2639-2658. https://doi.org/10.1016/j.istruc.2021.06.002.

BHRC, 2014. *Iranian Code of Practice for Seismic Resistant Design of Buildings (Standard 2800)*. Building and Housing Research Center, 4th Edition, Tehran, Iran. (In Persian). [Link]

Borcherdt, R. D., 1994. Estimates of site-dependent response spectra for design (methodology and justification). *Earthquake Spectra,* 10(4), 617-653. [Link]

Chadha, R. K., Singh, C. and Shekar, M., 2008. Transient changes in well-water level in bore wells in Western India due to the 2004 M w 9.3 sumatra earthquake. *Bulletin of The Seismological Society of America*, 98(5), 2553-2558. [Link]

Chitte, C. J., Charhate, S. and Mishra, S. S., 2022. Seismic performance of RC elevated water storage tanks. *Materials Today: Proceedings*, 65(2), 901-907. https://doi.org/10.1016/j.matpr.2022.03.523.

Danciu, L., Şeşetyan, K., Demircioglu, M., Gülen, L., Zare, M., Basili, R. et al., 2018. The 2014 earthquake model of the Middle East: seismogenic sources. *Bulletin of Earthquake Engineering*, 16(8), 3465-3496. https://doi.org/10.1007/s10518-017-0096-8.

Eidinger, J., De Castro, L. and Ma, D., 2006. The 1906 earthquake impacts on the San Francisco and Santa Clara water systems-what we learned, and what we are doing about it. *Earthquake Spectra*, 22(2_suppl), 113-134. https://doi.org/10.1193/1.2186986.

Eshghi, S., Zare, M., Nasserasadi, K. S., Razzaghi, M. N., Ahari, M. and Motamedi, M., 2004. Reconnaissance report on Dec. 26, 2003, Bam (Iran) earthquake. International Institute of Earthquake Engineering and Seismology (IIEES), Ministry of Science, Research and Technology, Tehran, Iran. (In Persian). [Link]

Eskandari, M., Darabi, M. and Ranjbar, F., 2024. Vulnerability assessment of the water network by considering the interdependency with other critical infrastructures-case study: the water network of Neyshabour City. *Journal of Water and Wastewater*, 34(6), 39-54. https://doi.org/10.22093/wwj.2024.437058.3396.

Eskandari, M., Omidvar, B., Modiri, M. and Nekooie, M. A., 2020. Model for earthquake damage analysis in lifeline utility systems with consideration of uncertainties. *Journal of Infrastructure Systems*, 26(3), 05020005. https://doi.org/10.1061/(ASCE)IS.1943-555X.0000547.

Esposito, S., Giovinazzi, S., Elefante, L. and Iervolino, I., 2013. Performance of the L'Aquila (central Italy) gas distribution network in the 2009 (M_w 6.3) earthquake. *Bulletin of Earthquake Engineering*, 11(6), 2447-2466. https://doi.org/10.1007/s10518-013-9478-8.

Fakhimi, B. and Rahemi, A. A., 2014. *Vulnerability Assessment Studies, Earthquake Improvement Plans (Horizontal and Vertical Earthquake Components), and Retrofitting of on-Ground Concrete Water Tanks in Kashan City*. Report on Research Project, Islamic Azad University, Kashan, Iran. (In Persian). [Link]

Fallah-Aliabadi, S., Ostadtaghizadeh, A., Ardalan, A., Eskandari, M., Fatemi, F., Mirjalili, M. R. et al., 2020. Risk analysis of hospitals using GIS and HAZUS: a case study of Yazd County, Iran. *International Journal of Disaster Risk Reduction*, 47, 101552. https://doi.org/10.1016/j.ijdrr.2020.101552.

FEMA, 2022. *Hazus Earthquake Model Technical Manual*. HAZUS 5.1, Federal Emergency Management Agency, USA. [Link]

Fragiadakis, M., Christodoulou, S. E. and Vamvatsikos, D., 2013. Reliability assessment of urban water distribution networks under seismic loads. *Water Resources Management*, 27(10), 3739-3764. https://doi.org/10.1007/s11269-013-0378-0.

Ghadimi Chermahini, A. and Tahghighi, H., 2019. Numerical finite element analysis of underground tunnel crossing an active reverse fault: a case study on the Sabzkouh segmental tunnel. *Geomechanics and Geoengineering*, 14(3), 155-166. https://doi.org/10.1080/17486025.2019.1573323.

Gopisetti, L. S. P., Ceylan, H., Kim, S., Cetin, B. and Kaya, O., 2021. Sensitivity index comparison of pavement mechanistic-empirical design input variables to reflective cracking model for different climatic zones. *Road Materials and Pavement Design*, 22(10), 2232-2247. https://doi.org/10.1080/14680629.2020.1747523.

Hou, B., Jia, R., Wu, B., Liu, L. and Xu, C., 2026. Seismic resilience assessment of water treatment plants considering the damages and interdependencies of internal facilities. *Soil Dynamics and Earthquake Engineering*, 201, 109934. https://doi.org/10.1016/j.soildyn.2025.109934.

Huang, F., Chen, Y., Ji, P., Ren, K., Gao, F. and Zhang, L., 2015. Co-seismic changes of well water level and volume strain meter in capital area and its vicinity, due to the Nov.14, 2001 Ms8.1 Kunlun Mountain earthquake, China. *Geodesy and Geodynamics*, 6(6), 460-466. https://doi.org/10.1016/j.geog.2015.12.005.

Ilyati, I. and Akbari, M., 2024. Flood risk zoning in vulnerable components of the water supply system of Kashan City. *Journal of Water and Wastewater*, 35(4), 113-131. (In Persian). https://doi.org/10.22093/wwj.2025.502819.3463.

Jamali, F., Hessami, K. and Ghorashi, M., 2011. Active tectonics and strain partitioning along dextral fault system in Central Iran: analysis of geomorphological observations and geophysical data in the Kashan region. *Journal of Asian Earth Sciences*, 40(4), 1015-1025. https://doi.org/10.1016/j.jseaes.2010.05.013.

JICA, 2006. *The Study on The Water Supply System Resistant to Earthquakes in Tehran Municipality in The Islamic Republic of Iran*. Japan International Cooperation Agency: Nihon Suido Consultants Co., Ltd. and Tokyo Engineering Consultants Co., Ltd. Japan. [Link]

Kashan Water and Wastewater Engineering Company, 2017. *Geotechnical Investigations Report*. Technical and Soil Mechanics Laboratory Department of Isfahan Province, Isfahan, Iran. (In Persian). [Internal document]

Kennedy, R. P., Cornell, C. A., Campbell, R. D., Kaplan, S. and Perla, H. F., 1980. Probabilistic seismic safety study of an existing nuclear power plant. *Nuclear Engineering and Design*, 59(2), 315-338. https://doi.org/10.1016/0029-5493(80)90203-4.

Kim, Y. S., Spencer Jr, B. F., Song, J., Elnashai, A. S. and Stokes, T., 2007. *Seismic Performance Assessment of Interdependent Lifeline Systems*. Mid-America Earthquake Center, USA. 1-39. [Link]

Li, J. and Ni, P., 2025. Fragility analysis of buried continuous pipelines under normal faulting through analytical solution combining with machine learning technique. *Canadian Geotechnical Journal*, 62, 1-18. https://doi.org/10.1139/cgj-2024-0430.

Liu, W., Xie, Z. and Xie, J., 2025. Seismic reliability assessment of in-service water distribution networks. *Probabilistic Engineering Mechanics*, 81, 103826. https://doi.org/10.1016/j.probengmech.2025.103826.

Melissianos, V. E., Vamvatsikos, D., Danciu, L. and Basili, R., 2024. Design displacement for lifelines at fault crossings: the code-based approach for Europe. *Bulletin of Earthquake Engineering*, 22(5), 2677-2720. https://doi.org/10.1007/s10518-023-01813-9.

Melville, C. P. and Ambraseys, N. N., 2005. *A History of Persian Earthquakes*. Cambridge University Press, England. 240 pages. [Link]

Moinfar, A. A., Naderzadeh, A. and Nabavi, M. H., 2012. New Iranian seismic hazard zoning map for new edition of seismic code and its comparison with neighbor countries. *15th WCEE LISBOA, 1-10*. Lisbon, Portugal. [Link]

Municipality of Kashan, 2015. *Geotechnical Investigations Report*. Soil Mechanics Laboratory, Islamic Azad University, Kashan, Iran. (In Persian). [Internal document]

FEMA, 1997. *Earthquake Loss Estimation Methodology-HAZUS: Technical Manual, Volume 2*. Federal Emergency Management Agency, Pennsylvania State University. USA. [Link]

Pavel, F., Vacareanu, R., Arion, C., Aldea, A. and Scupin, A., 2021. Seismic risk assessment of lifelines in Bucharest. *International Journal of Disaster Risk Reduction*, 66, 102629. https://doi.org/10.1016/j.ijdrr.2021.102629.

Pires, H., Rodrigues, H., Afonso, A. S., Pimentel-Rodrigues, C. and Rodrigues, F., 2020. Seismic vulnerability assessment of a water supply network: city of Aveiro case study. *Proceedings of the 2nd International Workshop on Natural Hazards (NATHAZ'19), Pico Island-Azores 2019.* Portugal. Springer, Cham. pp. 27-31. [Link]

Pitilakis, K., Alexoudi, M., Argyroudis, S., Monge, O. and Martin, C., 2006. Earthquake risk assessment of lifelines. *Bulletin of Earthquake Engineering*, 4(4), 365-390. https://doi.org/10.1007/s10518-006-9022-1.

Pitilakis, K., Alexoudi, M., Argyroudis, S., Monge, O. and Martin, C., 2008. Vulnerability and Risk Assessment of Lifelines. In: Oliveira, C. S., Roca, A., Goula, X. Eds. *Assessing and Managing Earthquake Risk*. Geotechnical, Geological and Earthquake Engineering. Springer, Dordrecht. pp. 185-211. https://doi.org/10.1007/978-1-4020-3608-8_9.

Pitilakis, K. and Argyroudis, S., 2014. Systemic seismic vulnerability and risk analysis of urban systems, lifelines and infrastructures. *Proceedings of the International Conference on Seismic Design of Industrial Facilities (SeDIF-Conference)*. Springer Fachmedien Wiesbaden, Germany. pp. 209-234. https://doi.org/10.1007/978-3-658-02810-7_18.

Porter, K. and Ramer, K., 2012. Estimating earthquake-induced failure probability and downtime of critical facilities. *Journal of Business Continuity and Emergency Planning*, 5(4), 352-364. https://doi.org/10.69554/unue6649.

Renovation Administration of Isfahan Province Schools, 2023. *Geotechnical Investigations Report*. Technical and Soil Mechanics Laboratory Department of Isfahan Province, Isfahan, Iran. (In Persian). [Internal document]

Rimal, H., Pradhan, P., Gautam, D. and Rupakhety, R., 2023. Seismic fragility of aging elevated water tank with smooth bars considering soil structure interaction. *Buildings*, 13(1), 4. https://doi.org/10.3390/buildings13010004.

Scawthorn, C., Miyajima, M., Ono, Y., Kiyono, J. and Hamada, M., 2006. Lifeline aspects of the 2004 Niigata ken Chuetsu, Japan, Earthquake. *Earthquake Spectra*, 22(1_suppl), 89-110. [Link]

Şeşetyan, K., Danciu, L., Demircioğlu Tümsa, M. B., Giardini, D., Erdik, M., Akkar, S. et al., 2018. The 2014 seismic hazard model of the Middle East: overview and results. *Bulletin of Earthquake Engineering*, 16(8), 3535-3566. https://doi.org/10.1007/s10518-018-0346-4.

Pitilakis, K., Crowley, H. and Kaynia, A. M., 2014. SYNER-G: Typology Definition and Fragility Functions for Physical Elements at Seismic Risk. In Ansal, A., Bommer, J., Bray, J. B., Pitilakis, K., Yasuda, S., Eds., *Geotechnical, Geological and Earthquake Engineering*, pp. 221-258. [Link]

Tabaei, M., Mehdizadeh, R. and Esmaeili, M., 2016. Stratigraphical evidences of the Qom-Zefreh fault system activity, Central Iran. *Journal of Tethys*, 4(1), 018-026. [Link]

Tahghighi, H., 2011. Earthquake fault-induced surface rupture-a hybrid strong ground motion simulation technique and discussion for structural design. *Earthquake Engineering and Structural Dynamics*, 40(14), 1591-1608. https://doi.org/10.1002/eqe.1105.

Tahghighi, H. and Ghafoori, S. M. M., 2023. *Risk Assessment of Kashan Water and Wastewater Systems Subjected to Earthquake Hazard*. Report on research project, Grant-in-aid for scientific research, University of Kashan, Kashan, Iran. (In Persian). [Link]

Tavasoli, S., Sotudeh, A. S. and Bakhshi, A., 2022. Shaking table test for assessing the seismic performance of semi-anchored steel water tanks. *Thin-Walled Structures*, 176, 109311. https://doi.org/10.1016/j.tws.2022.109311.

Tehran Padir Consultant Engineering, 2012. *A Comprehensive Report for Seismic Microzonation and Vulnerability of Kashan, Iran*. Isfahan Housing and Urban Development Organization, Isfahan, Iran. (In Persian). [Internal document]

Terzic, V. and Villanueva, P. K., 2021. Method for probabilistic evaluation of post-earthquake functionality of building systems. *Engineering Structures*, 241, 112370. https://doi.org/10.1016/j.engstruct.2021.112370.

Toprak, S., Wham, B. P., Nacaroglu, E., Ceylan, M. and Dal, O., 2025. Performance of water systems during the February 6th Kahramanmaras earthquakes. *Earthquake Spectra*, 41(1), 322-353. https://doi.org/10.1177/87552930241293571.

Toprak, S., Wham, B. P., Nacaroglu, E., Sakamoto, M., Tunc, S. C., Davis, C. A. et al., 2026. Assessment of infrastructure failures in the 2023 Kahramanmaras Earthquakes. *ASCE OPEN: Multidisciplinary Journal of Civil Engineering*, 4(1), 04026001. https://doi.org/10.1061/AOMJAH.AOENG-0103.

Uma, S. R., Scheele, F., Abbott, E. and Moratalla, J., 2021. Planning for resilience of water networks under earthquake hazard: a case study for Rotorua District, New Zealand. *Bulletin of the New Zealand Society for Earthquake Engineering*, 54(2), 135-152. https://doi.org/10.5459/bnzsee.54.2.135-152.

Wen, P. and Bi, X., 2025. Spatial variation analysis for ground motions based on regional site conditions and separation distance. *Journal of Earthquake and Tsunami*, 19(04), 2550003. https://doi.org/10.1142/S1793431125500034.

Wu, H., Guo, E., Yan, P. and Liu, J., 2023. A quantitative evaluation model for the seismic resilience of water supply systems based on fragility analysis. *Sustainability*, 15(16), 12137. https://doi.org/10.3390/su151612137.